Heat transfer from a vertical tube bundle under natural circulation conditions

K. P. Hallinan and R. Viskanta*

A rectangular loop (thermosyphon) was used to measure the average heat transfer coefficients for water at atmospheric pressure under natural circulation conditions. A twenty-one tube bundle with tubes 1.65 m long and 9.55 mm in diameter, and a pitch-to-diameter ratio of 1.33, was used as a test heat exchanger in one of the vertical legs of the loop. A natural circulation flow in the loop developed due to buoyancy differences of the fluid in its two vertical legs. Flow visualization experiments were performed to determine the flow regimes associated with natural circulation flow longitudinal to a tube bundle. Empirical correlations for the average Nusselt number have been developed and are reported. Grid spacers arranged on tube bundles were shown to enhance heat transfer, especially for laminar flow, without any noticeable increase in pressure drop.

Keywords: *thermosyphon, natural circulation loop, combined convection, tube bundles*

Natural circulation loops (thermosyphons), created by heat addition and removal from a fluid in different parts of the system, arise in many engineering applications including process industry, solar heating and cooling systems, geothermal power generation, computer cooling, and some cooling modes of nuclear reactors. In the loop there is fluid flow due to buoyant forces that result from density differences between the heated and cooled parts of the loop. General reviews of thermosyphons including applications are available[1-4].

There are mainly two classes of problems of interest in various applications. The first is concerned with the heat removal or addition to the system and the steady-state performance of the system. The second problem deals with the stability of the system. Unstable flows are of concern where heat must be removed from the system, such as nuclear reactor core cooling, where flow reversals and flow stagnation can cause undesirable local temperature increases. Up-to-date literature reviews on mathematical modelling and stability of natural circulation loops are available[5,6]. A one-dimensional analysis is usually employed, where the only space coordinate runs around the circulation loop. Most of the available theoretical approaches to natural circulation have treated a single loop or lumped parallel branches into a single equivalent loop.

Often in applications, tube bundles are used to provide the source of heat addition and/or removal in a natural circulation loop. For example, in a nuclear reactor where the core consisting of a large number of fuel rods acts as the heat source in the system, the natural circulation flow is not only important to the cooling of the reactor core during shutdown but also when forced coolant flow is interrupted. Therefore, in order to model the dynamic and steady-state performance not only of nuclear reactor cooling but also of industrial and solar energy utilization systems, it is essential to understand heat transfer from the tube bundle to the circulating fluid.

Previous work on heat transfer is natural circulation loops is applicable only to the particular geometry of the loop in each study and to the type of heat input to the system. No general conclusions can be drawn from the studies reported. Specifically, very little work has been performed on loops where tube bundles are used to provide the source of heat addition and the sink for heat removal. Gruszczynski and Viskanta[7] have performed experiments using a bundle with a triangular tube array as the source of heat in a vertical leg of a closed rectangular loop. They developed empirical correlations for the average Nusselt number and friction factor applicable to the bundle

No other known work provides such correlations for natural convection circulation along tube bundles. Zvirin *et al*[8] have conducted experiments to study the effects of core flow resistance and power distribution modelling a typical pressurized water reactor. Also, for a toroidal loop, Damerell and Schoenhals[9] have developed heat transfer and fluid friction correlations.

While the results for natural circulation flows are limited, forced flow results are documented for a wide range of tube bundle geometries. Sparrow and Loeffler[10] have analysed longitudinal, fully developed, laminar flow between cylinders to determine pressure drop and friction factors for arrays with different porosities. Also, for laminar forced flow, Schmid[11] has presented an analysis showing that, except for small pitch-to-diameter ratios, each individual tube could be considered isolated from the other tubes. All correlations should then be based on this 'effective flow area' about one tube. Mohanty and Roy[12] have found that the experimental data for the friction factor in laminar flow could be accurately represented by Blasius type correlations using the hydraulic diameter of one tube based on the effective flow area. Up-to-date reviews of fluid friction and heat transfer data for low

* Heat Transfer Laboratory, School of Mechanical Engineering, Purdue University, West Lafayette, IN 47907, USA
Received 27 February 1985 and accepted for publication on 8 June 1985

Reynolds number, forced convection flow are available[13,14].

In many pwr (pressurized water reactor) fuel assemblies, in-tube bundle grid spacers are used to separate the rods and tubes, and it is essential to know their effect on heat transfer and pressure drop. Much work has been done in this respect for forced flow conditions, but none appears to have been reported for natural circulation flows. Previous results[15-17] indicate that the blockage in the flow created by the grid spacers increases the pressure drop and enhances the heat transfer due to mixing in the region of the spacer.

This paper describes natural circulation flow and heat transfer experiments along a vertical tube bundle. Flow patterns and regimes under natural circulation conditions were observed using flow visualization techniques. Empirical correlations for the average heat transfer coefficients and fluid friction factors under steady-state natural circulation flow conditions were developed. The effect of grid spacers on flow patterns, fluid friction, and heat transfer were also determined.

Experimental apparatus

Natural circulation loop

The single-phase natural circulation loop used in the experiments is shown schematically in Fig 1. The loop is constructed from Kimax glass tubing and contains two tubular heat exchangers and associated instrumentation. The inside diameter of the glass tubing is 7.62 cm. To ensure that the manufacturer's specification for the safe pressure of the glass loop is not exceeded during operation, a reservoir open to the atmosphere is fitted to one of the top flanges, allowing for normal operation of the loop at atmospheric pressure. The loop is insulated

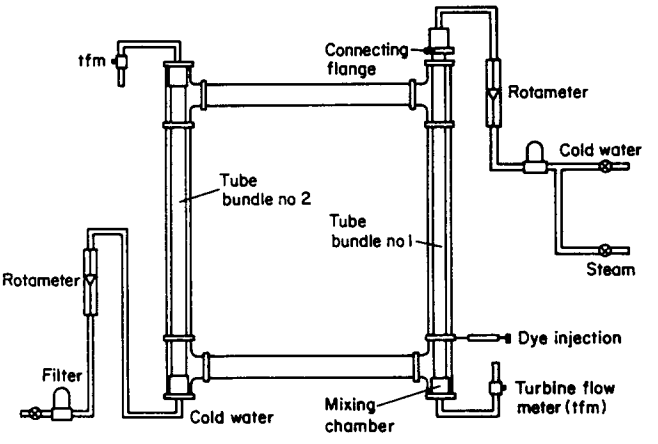

Fig 1 Schematic diagram of the experimental natural circulation loop

with three layers of 2.54 cm thick Johns-Manville insulation tubing on the vertical and horizontal legs as well as on each of the tees.

The two tube bundles shown in Fig 1 provide a means for heat addition and removal using water as the working fluid. The tube bundle (No 1) serves as the heat source in the natural circulation loop, whereas the other tube bundle (No 2) serves as the heat sink. The inlets and outlets to each of the tube bundles could be interchanged, allowing for the possibility of using each of the tube bundles as heat exchangers in both counter-flow and parallel-flow arrangements. Dimensions and characteristics of each tube bundle are given in Table 1.

Tube bundle No 1 was constructed of a cluster of twenty-one copper tubes 1.65 m in length arranged in a rectangular array, having tube diameters of 9.55 mm and a pitch-to-diameter ratio (pdr) of 1.33. Tube bundle No 2

Notation

A	Cross-sectional flow area of loop components, defined by Eq (9)
c	Specific heat
D_h	Hydraulic diameter $=4A_f/P_{ht}$ or $4A_f/P_{sh}$
D_t	Inside diameter of loop tube
f	Friction factor
G	Mass flow rate of circulating fluid
Gr	Grashof number $=\rho^2 g\beta\,\Delta T_{w-L} D_h^3/\mu^2$
Gr_m	Modified Grashof number $=\rho^2 g\beta q_{so} D_h^4/k\mu^2$
g	Gravitational constant
$\bar{h}$	Average heat transfer coefficient
K	Form loss coefficient
k	Thermal conductivity
L	Length of tube bundle in source leg
$\dot{m}$	Mass flow rate of fluid passing through tube bundles
$\overline{Nu}$	Average Nusselt number on outside of tubes
n	Number of tubes in a heat exchanger bundle
P	Perimeter
P_{ht}	Heat transfer perimeter $=nxd_0$
P_{sh}	Shear perimeter $=P_{ht}+2\pi D_t$
Pr	Prandtl number
q_{so}	Average heat flux to the circulating fluid in the source leg of the loop
R	Effective flow resistance, Eq (2)
Re	Reynolds number $=GD_h/A\mu$
S	Pitch (spacing) of tubes in bundle
s	Spatial coordinate about the loop
U	Overall heat conductance of loop tube and insulation
T	Local temperature
β	Thermal expansion coefficient of water
ε	Porosity of tube bundle
ΔT_D	Average temperature difference of the circulating fluid between the two vertical legs of the loop $=\int_0^L [T_{so}(x)-T_{si}(x)]\,dx/L$
ρ	Density of fluid or loop structural components
ρ_0	Density of circulating fluid at reference temperature
μ	Dynamic viscosity of fluid

Subscripts

a	Refers to the ambient
f	Refers to the circulating fluid in the loop
ins	Refers to the insulation
i	Refers to the fluid passing through the tube bundle
t	Refers to the loop tubing
w	Refers to the tube walls in the bundle
si	Refers to sink leg
so	Refers to source leg

Table 1 Dimensions and characteristics of the tube bundles and loop

Dimensions	Tube bundle No 1	Tube bundle No 2
No of tubes	21	7
od of tubes, mm	9.55	19.05
Tube thickness, mm	1.587	1.02
Length of tube bundle, mm	1.6515	1.575
Cross-sectional flow area, m^2	0.003064	0.002565
Type of array	Rectangular	Triangular
Pitch-to-diameter ratio	1.33	1.25
Hydraulic diameter, m (heat transfer)	0.0195	0.0245
Hydraulic diameter, m (shear area)	0.0141	0.0156
Hydraulic diameter, m (equiv. flow area)	0.012	0.0138
Length of horizontal legs of loop, m	1.486	1.486
Length of vertical legs of loop, m	1.499	1.499
Total volume of water in loop, m^3	0.2145	0.2145
Porosity (area of bundle/area of loop leg)	0.67	0.57

was constructed of seven copper tubes arranged in a triangular array with a pdr of 1.25. The arrangement shown for tube bundle No 1 was chosen because the array is similar in geometry to pwr fuel bundles.

Heating and cooling fluid was supplied by cold and hot water lines along with a high pressure steam line. The cooling fluid was supplied by a cold water line at a temperature of $14 \pm 1°C$.

Instrumentation

The loop was instrumented so that heat addition and removal from the loop could be determined from the measured working fluid temperature changes over the length of the tube bundles and the mass flow rates of the working fluid through the tube bundles. The mass flow rate of the circulating fluid was determined from an energy balance on the loop and the tube bundles at steady-state conditions. As a result of the low velocities of the circulating fluid in the loop, invasive methods could not be used for the measurement of the local velocity without disturbing the flow field. Optical methods such as ldv could be used for such a purpose, but the technique is also frought with difficulties such as a precise location of the test volume in a fluid which has large temperature gradients and a rather strong variation of the index of refraction with temperature.

The loop was instrumented with copper constantan thermocouples. On tube bundle No 1, six thermocouples were placed on the outside wall of the central tube to measure the wall temperature along the length of this tube. Three thermocouples were placed on the outside wall of a tube adjacent to the central tube, and two thermocouples were placed on the outside wall of one of the outer tubes. The off-centre tubes were instrumented to determine if any differences in wall temperature between the central and outer tubes was evident. Similarly, seven thermocouples were soldered to tube bundle No 2: five along the central tube and two on one of the outer tubes.

In addition to these thermocouples, a differential thermocouple was set up across each tube bundle to measure accurately the temperature difference of the heating/cooling fluid across the tube bundles. Also, in each header of both tube bundles, copper-constantan thermocouples were installed to measure directly the temperature of the fluid at the inlets and outlets of the heat exchangers. Thermocouples were installed on both ends of each of the horizontal connecting legs to measure an approximate bulk mixed mean temperature (within experimental error) of the circulating fluid in the loop at each cross-section. The wall temperatures of the containment tubing were measured by installing eight thermocouples along the outer wall of the tubing at various locations around the loop. Fig 2 shows the locations of all thermocouples on the loop.

The heating and cooling average fluid flow rates were measured using Brooks turbine flow meters, which produce a number of pulses proportional to the flow rate. The pulses were recorded by two Anadex digital counters.

The fluid flow was visualized by injecting a fluorescent dye (flourescein disodium salt) into the circulating fluid. A flange connecting the lower tee to the vertical leg of the glass loop on the side of the heat source was modified to allow for dye injection with a syringe.

Test procedure

The loop was filled with deionized water. The copper tube heat exchangers in the source and sink legs were connected to the heating and cooling fluid lines, respectively. The valves controlling the flow in the heating

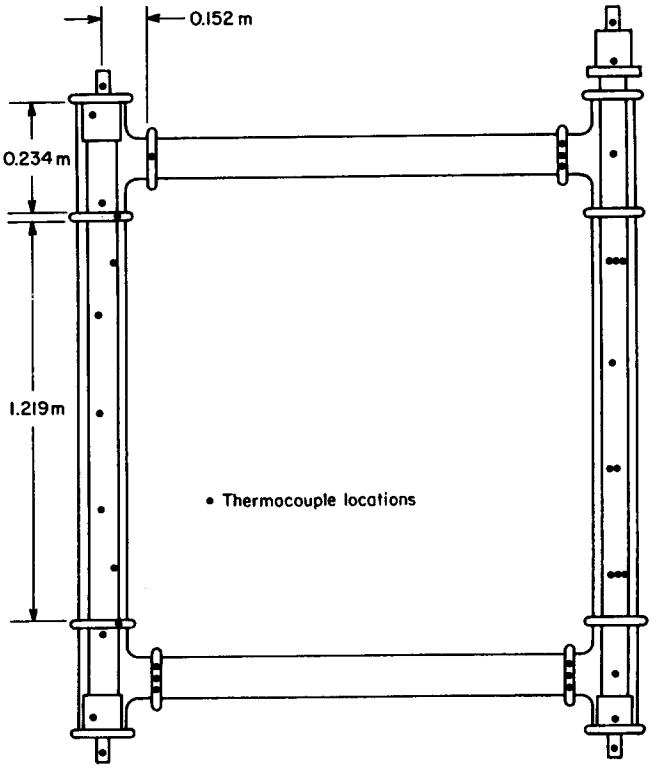

Fig 2 Location of thermocouples in the loop

and cooling fluid lines were opened to initiate flow of the working fluid through the heat exchangers. The temperature of the heating fluid was controlled by changing the rate at which steam was mixed with cold water. The flow rates of the fluid passing through both heat exchangers could easily be controlled by adjusting the gate values in both lines, and were constant (within $\pm 5\%$) for the test runs.

A series of steady-state tests were run in succession to assure similar ambient conditions for each set of tests. Steady-state conditions were reached when all the temperatures monitored showed no change, except for fluctuations over a period of 5 minutes. A typical steady-state run consisted of fifteen to sixteen tests at different heating rates.

Readings were recorded and averaged over 5-minute intervals because of temperature and flow rate fluctuations. Ten temperature readings at 30 s intervals were taken at each condition and averaged. An average value of the pulses per second from the turbine flow meters was obtained from the total number of pulses over this time period.

A similar series of steady-state tests was performed after egg-crate type grid spacers had been arranged on tube bundle No 1. A total of four grid spacers were inserted over tube bundle No 1, spaced at intervals of 53 cm. A schematic diagram of the spacer grids is shown in Fig 3.

Analysis

Physical model and assumptions

When the hot and cold vertical legs of a natural circulation loop are connected as in Fig 1, the flow in one communicates with the other. A pumping action due to the difference in the average density in the two legs is present. This is the forced convection component. In other words, the phenomenon in the loop is forced convective, but locally in each of the vertical legs natural convection supports or opposes forced convection. Forced convection cannot occur if the two vertical legs are not connected, irrespective of the heat addition or removal.

A mathematical model has been developed to predict the thermal performance of a single-phase natural circulation loop, shown in Fig 1. A one-dimensional model, where the only space coordinate, s, runs along the components of the loop is adopted to describe the spatial dependence of the mass flow rate and temperature[4,8]. The temperature is, then, the cross-sectional average in each component of the loop.

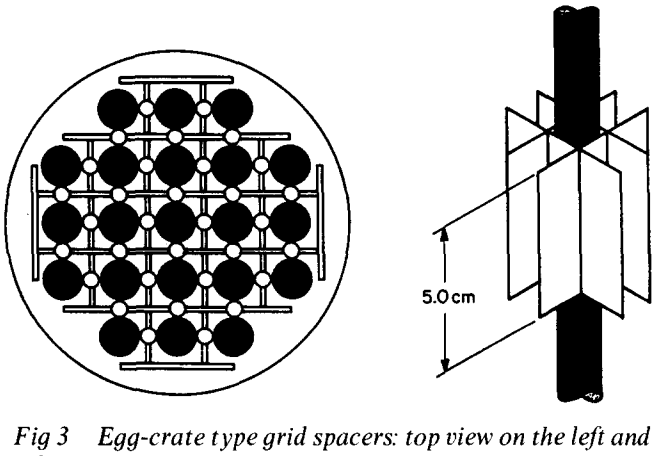

Fig 3 Egg-crate type grid spacers: top view on the left and side view on the right

To describe mathematically the thermal performance of a natural circulation loop, we apply the principles of conservation of mass, momentum and energy to a differential volume element of fluid or structural component. The Boussinesq approximation is adopted, ie the density of the fluid is considered constant in the governing equations except in the buoyancy term. The other fluid properties are assumed constant, which is justifiable for the small temperature variations expected. Separate energy balances are made on the working fluid, the tube bundle, the circulating tube, the loop piping and the insulation. Axial heat conduction (in the s-direction) along the internal structural components comprising the loop, as well as the circulating fluid, are neglected in comparison to advection or convection. Kinetic and potential energy changes of the circulating fluid are negligible in comparison to advection, and are ignored.

Mathematical model

Under steady-state conditions, and assuming that the circulating flow is incompressible, from the equation of mass conservation it is apparent that the mass flow rate of the circulating fluid is constant. Following the analysis of Zvirin[4], the momentum equations for each leg of the loop were integrated over their respective lengths. This yields the momentum equation for the entire loop:

$$RG^2/2\rho = \rho_0 g\beta L^2\left[\int_0^L T_{so}(s)\,\mathrm{d}x - \int_0^L T_{si}(s)\,\mathrm{d}x\right] = \rho_0 g\beta^2 L\,\Delta T_D \tag{1}$$

where ΔT_D is the average temperature difference of the circulating fluid between the two vertical legs of the loop, and R is the effective flow resistance parameter and is composed of the sum of the frictional and form losses,

$$R = \sum_i f_i \frac{L_i}{D_{hi}A_i^2} + \sum_j \frac{K_j}{A_j^2} \tag{2}$$

The energy equation must be written for each component of the indivual legs of the loop. For the vertical leg of the loop containing heat exchanger No 1, an energy equation was written for the fluid flowing through the tube bundle, the tube walls of the heat exchanger, the circulating fluid, the glass walls, and the insulation. Under steady state conditions the energy equations for the components become:

Working fluid

$$\dot{m}c\frac{\mathrm{d}T_i}{\mathrm{d}s} = h_i P_i n(T_w - T_i) \tag{3}$$

Tube bundle

$$h_i P_i n(T_i - T_w) - h_f P_f n(T_w - T_f) = 0 \tag{4}$$

Circulating fluid

$$Gc\frac{\mathrm{d}T_f}{\mathrm{d}s} = h_f P_f n(T_w - T_f) - U_t P_t (T_f - T_a) \tag{5}$$

The heat transfer rate to the circulating fluid is determined from Eq (3) from the knowledge of the

temperature difference and the mass flow rate of the water flowing through the heat exchangers. The mass flow rate of the circulating fluid is determined by equating the heat capacity rates of the fluid flowing through the test bundle and the circulating fluid passing axially over the bundle.

Local temperatures of the fluid flowing through the heat exchangers were calculated knowing the inlet and outlet temperatures for turbulent, hydrodynamically fully developed, thermally developing flow[18], and then adjusting a constant in a correlation for the convection heat transfer coefficient h_i so that a numerical solution of Eq (3) results in a calculated outlet temperature equalling the measured one.

Local heat transfer rates were calculated from the knowledge of the local heat transfer coefficients inside the tubes, the corrected local temperatures for the fluid flowing through the tubes, and the measured local tube wall temperatures.

An iterative procedure was used to determine both the local temperatures and local heat transfer coefficients for the circulating fluid. Initially, local temperatures for the circulating fluid in the source leg were assumed. Local values for the heat transfer coefficient on the outside of the tubes could then be determined from Eq (4). Then, from Eq (5), new values for the working fluid temperatures were determined based on the calculated values for the local heat transfer coefficients. This procedure was repeated until all of the local temperatures and heat transfer coefficients converged.

The hydraulic diameter used in the above development was defined as

$$D_h = 4A/P_{ht} \quad \text{or} \quad D_h = 4A/P_{sh} \tag{6}$$

The perimeter for shear and heat transfer, P_{sh}, and the perimeter for heat transfer, P_{ht}, are defined as

$$P_{sh} = n\pi d_o + \pi D_t \tag{7}$$

and

$$P_{ht} = n\pi d_o \tag{8}$$

For the tube bundles in each of the vertical legs, the hydraulic diameter is typically based on the equivalent flow area around one tube[10,11]. In a square array bundle, this flow area is

$$A = S^2 - \pi d_o^2/4 \tag{9}$$

where S is the pitch or spacing of the tubes in the bundle. The perimeter for heat transfer is simply the outer perimeter of one tube, assuming that heat transfer does not vary from tube to tube in the bundle.

Results and discussion

Steady-state tests in absence of grid spacers

The effect of the heat exchanger flow arrangement, heat exchanger flow rates, and heating rates on heat transfer and fluid friction for longitudinal natural circulation flow through a tube bundle was determined. Listed in Table 2 are the conditions for each of the tests.

Flow visualization and fluid friction

The flow was observed to be stable in all cases. Also, the circulating fluid flow rate was observed to increase/decrease almost instantaneously (within 5 seconds) after a step increase/decrease in the heating rate was implemented.

Flow visualization experiments showed a definite transition region from laminar to turbulent (mixed) flow. On the average, the transition from laminar turbulent flow occurred when

$$Gr = 6.6 \times 10^5, \qquad Gr_m = 4.8 \times 10^5, \qquad Re = 340$$

Fig 4 illustrates the relationship between the Reynolds number, Re, and the Grashof number, $Gr_{\Delta T_D}$, for the counter-flow and parallel-flow arrangements. Note that the Reynolds number is proportional to the mass flow rate of the circulating fluid in the loop, and the Grashof number, based on the driving temperature difference ΔT_D, is proportional to the heat addition to the system. The results show that for identical heat addition rates the mass flow rate of the circulating fluid in the

Table 2 Summary of steady-state tests

Data set	$\dot{m}$, kg/s of fluid		Tube bundle No 1 Arrangement
	Cooling	Heating	
A	0.050	0.15	Counter-flow
B	0.050	0.09	Counter-flow
C	0.090	0.15	Counter-flow
D	0.050	0.15	Parallel-flow
E	0.050	0.09	Parallel-flow
F	0.090	0.15	Parallel-flow

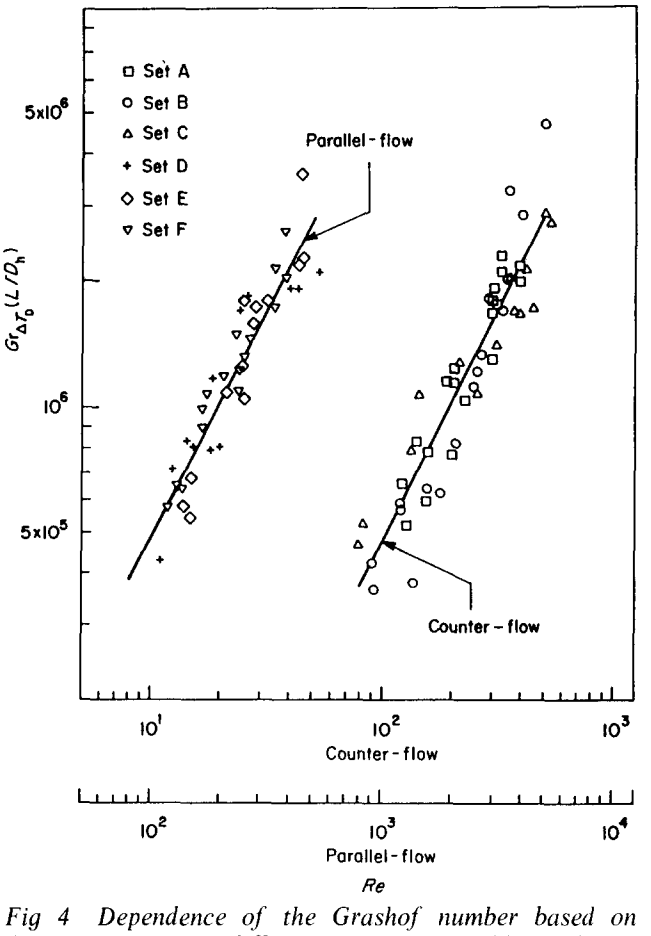

Fig 4 Dependence of the Grashof number based on driving temperature difference on the Reynolds number

parallel-flow arrangement is greater than for the counter-flow case. The explanation for this observation is that for parallel-flow a larger temperature difference between the heat exchanger fluid and the circulating fluid at the bottom of the source leg was measured than for the counter-flow case. This resulted in a larger buoyancy driving force, causing a higher mass flow rate of the circulating fluid.

Frictional pressure drop could not be determined experimentally using invasive methods, because the velocity of the circulating fluid was too small. Therefore, the frictional resistances in each of the component legs of the loop was determined indirectly. The analysis of the effective flow resistance parameter R indicates that a plot of RA_f^2 versus $1/Re$ would be a straight line of the form[7]

$$RA_f^2 = C_R/Re + K_T A_f^2 \tag{10}$$

where A_f is the cross-sectional flow area and Re is the Reynolds number of the circulating fluid in the source leg. The constant C_R is composed of the individual friction factors for each loop component, and K_T is the total form loss coefficient for flow in the loop. Analysis of the data indicates a slope of $C_R = 8050$ and $K_T A_f^2 = 1.467$. The intercept is nearly zero, indicating that the effect of form losses in the loop is negligible in comparison with the frictional losses.

From this value for C_R, the friction factor relations for the individual legs of the loop can be found. Assuming that in each of the legs the friction factor can be represented as $f = a/Re$, and taking the coefficients as $a_L = 43$ for the horizontal connecting legs[19], and assuming that $a_1 = a_2$ since the porosities of the two bundles are approximately equal[10], then $a_1 = a_2 = 31.2$. For forced convection laminar flow in a tube bundle with 19 tubes in a square array and $S/D = 1.3$ (approximately the same as the rod bundle used in this study) a_1 was found to be 27[12].

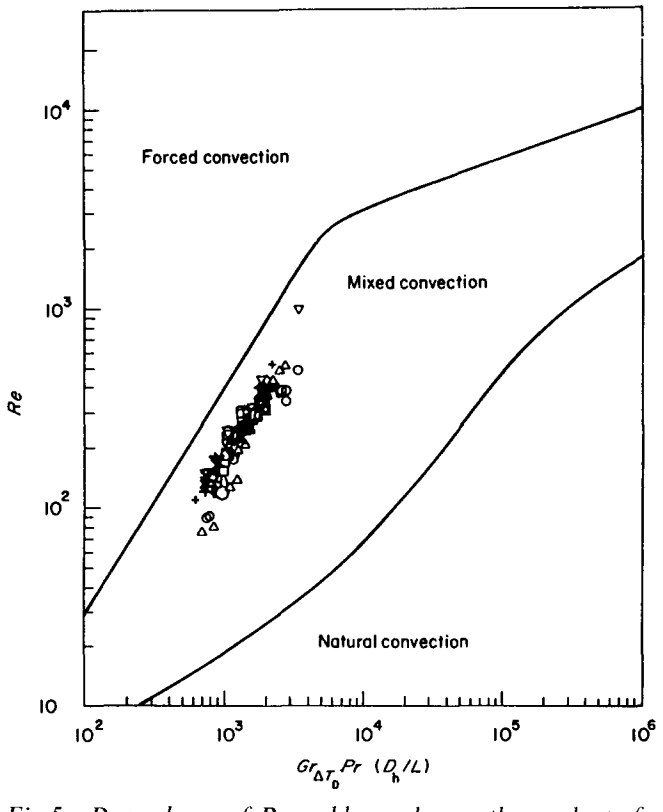

Fig 5 Dependence of Reynolds number on the product of Grashof and Prandtl numbers time the ratio of the hydraulic diameter to length of the source (flow regime boundaries after Ref 20)

To understand better the flow and heat transfer regimes under natural circulation conditions, a plot of Re vs $GrPr(D_h/L)$ was made and is shown in Fig 5. The various regimes of flow based on a correlation of these parameters for flow in a vertical pipe are described in the literature[20]. Using the hydraulic diameters in place of the tube diameters in both the Reynolds and Grashof numbers, the flow in the natural circulation loop is seen to fall within the mixed convection regime.

Mixed convection does in fact exist. Consider a packet of fluid, initially in the source leg as was used by Welander[21] to describe flow instabilities. Buoyancy differences between the source and the sink legs cause the packet to circulate about the loop. When the packet of fluid completes one revolution and returns to the source leg it will have gained momentum from the buoyancy forces. So, to the source leg it will appear that the packet of fluid has been forced into the leg. Yet, buoyancy forces would still exist to drive the flow, so the particle of fluid passing through the source leg will be subjected to both forced and free convection.

Average heat transfer coefficients

Since unique parameters which control heat transfer in a natural circulation loop (as do the Rayleigh number in free convection or the Reynolds number in forced convection) have not been identified, different dimensionless parameters were tried in correlating the average Nusselt number data. For all attempts it was found that a better correlation could be obtained by plotting against $\overline{Nu}/Pr^{0.43}$ rather than the average Nusselt number, $\overline{Nu}$, alone. This finding is consistent with the results of a previous work[7].

Fig 6 shows a plot of the heat transfer parameter $\overline{Nu}/Pr^{0.43}$ vs the Reynolds number for both counter-flow and parallel-flow arrangements. For counter-flow a correlation determined on the basis of least squares fit of the data was of the form

$$\overline{Nu} = 0.026 Re^{0.93} Pr^{0.43} \tag{11}$$

For parallel-flow the following correlation was obtained,

$$\overline{Nu} = 0.051 Re^{0.80} Pr^{0.43} \tag{12}$$

The dashed lines in each of the figures represent results of Gruszczynski and Viskanta[7] for a different tube bundle geometry. The difference between the two correlations demonstrates the dependence of the heat transfer coefficient on the geometry of the tube bundle. The reason the average heat transfer coefficient data correlate vs the Reynolds number is because the Grashof number ($Gr_{\Delta T_D}$) is nearly proportional to the Reynolds number (see Fig 4).

In general, the parallel-flow arrangement resulted in higher Nusselt numbers than the counter-flow case for Reynolds numbers below 200. For increasing Reynolds numbers, the average Nusselt number for the counter-flow arrangement becomes progressively greater than that for the parallel-flow case. It appears that the buoyancy driving force for Reynolds numbers greater than 200 becomes progressively greater for the counter-flow case (Fig 4).

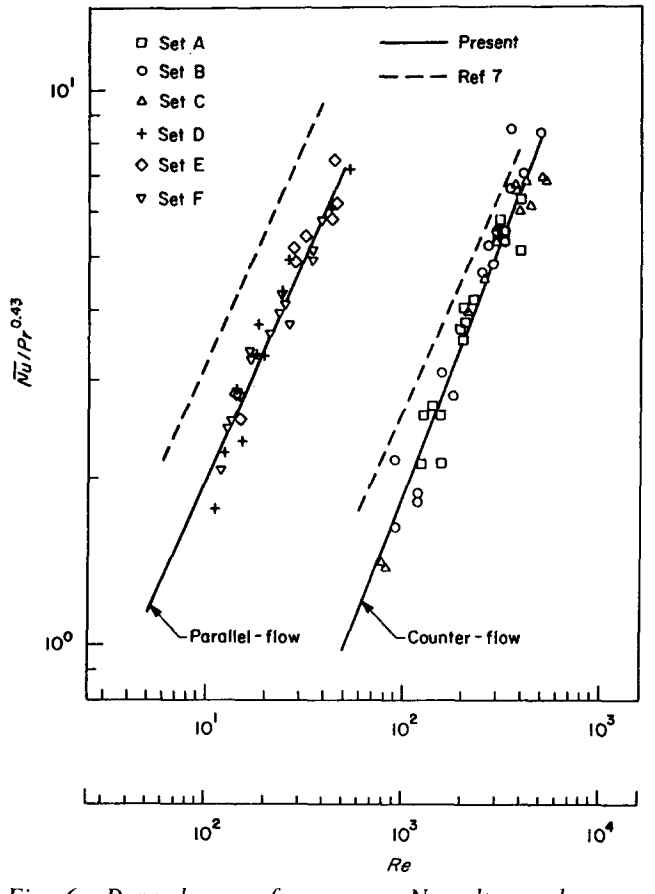

Fig 6 Dependence of average Nusselt number on Reynolds number

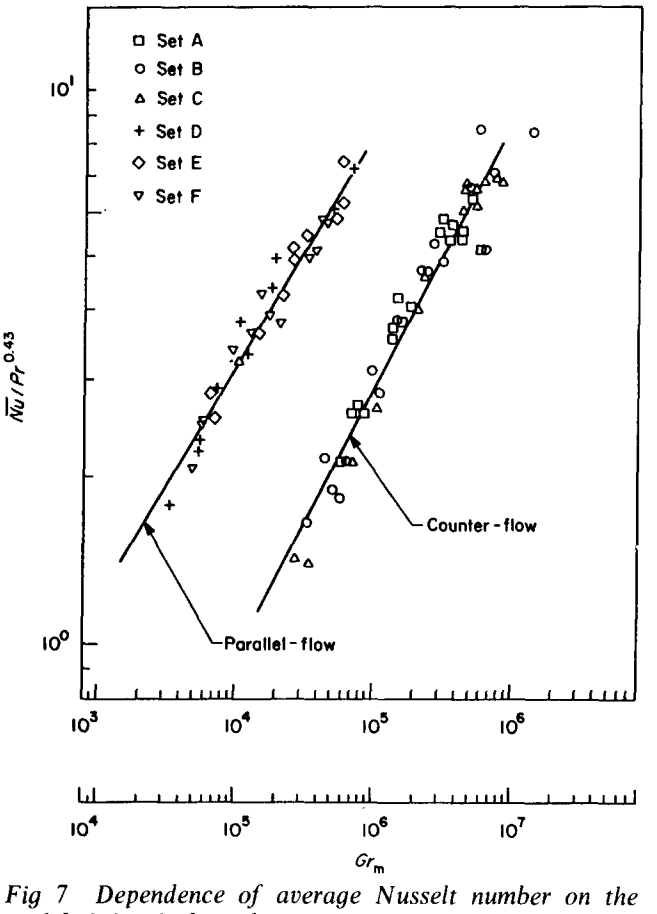

Fig 7 Dependence of average Nusselt number on the modified Grashof number

Another correlation for both the parallel-flow and counter-flow arrangement results from plotting $\overline{Nu}/Pr^{0.43}$ versus the modified Grashof number. Fig 7 shows the plots of $\overline{Nu}/Pr^{0.43}$ versus Gr_m for both flow arrangements. For counter-flow the correlation obtained from the least squares fit of the data is of the form:

$$\overline{Nu} = 0.11 Gr_m^{0.48} Pr^{0.43}, \qquad 4 \times 10^4 < Gr_m < 10^6 \qquad (13)$$

For parallel flow a similar correlation results in

$$\overline{Nu} = 0.024 Gr_m^{0.42} Pr^{0.43}, \qquad 4 \times 10^4 < Gr_m < 10^6 \qquad (14)$$

Attempts to correlate $\overline{Nu}/Pr^{0.43}$ vs the Grashof number Gr resulted in much more scatter. Note that the exponent on the Rayleigh (Grashof) number is considerably larger than that usually expected for laminar or turbulent natural convection conditions[19]. The dependence of the average Nusselt number on the Rayleigh number resembles that for natural convection in porous media for which $\overline{Nu} \propto Ra^m$, where m ranges between 0.5 and 0.69[22]. A similar type of Rayleigh number dependence was noted earlier for tubes in a triangular array[7].

Since mixed convection heat transfer appears to be prevalent in the natural circulation loop, an appropriate correlation of the average Nusselt number would be in terms of both the forced and natural convection parameters, the Reynolds and Grashof numbers, respectively. Since a correlation had been obtained for the average Nusselt number vs the Reynolds number to the 0.8 power for both flow arrangements, a plot of the Nusselt number times the Reynolds number to the 0.8 power divided by the Prandtl number to the 0.43 power versus the modified Grashof number was made, and is shown in Fig 8. It is apparent from this figure that the data

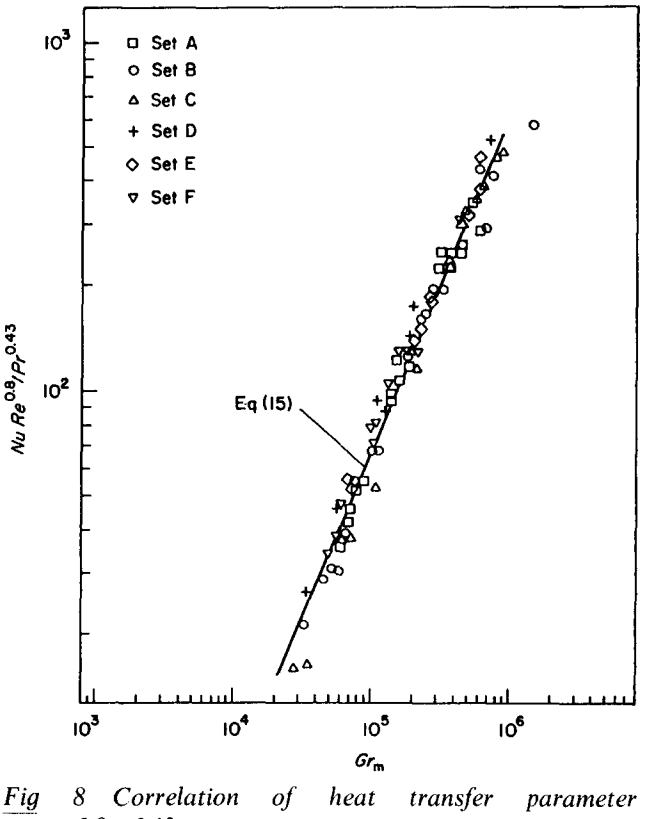

Fig 8 Correlation of heat transfer parameter $\overline{Nu}/Re^{0.8}Pr^{0.43}$ *with modified Grashof number*

from both the parallel-flow and counter-flow tests can be represented by a single curve, as given by the following correlation:

$$\overline{Nu} = 0.00091(Gr_m/Re)^{0.8} Gr_m^{0.176} Pr^{0.43} \quad (15)$$

The success of Eq (15) in correlating all of the experimental data suggests that, indeed, heat transfer under natural circulation conditions over a tube bundle is of the mixed convection type. The average Nusselt number is a function of both the Reynolds and Grashof numbers.

Heat transfer coefficients for a bundle with spacers

A set of steady-state experiments similar to those listed in Table 2 was performed after the egg-crate type spacers shown in Fig 3 were arranged on the test bundle. Only the effect of varying the heating rates was studied for each of the runs.

Flow visualization with the grid spacers arranged on the bundles did not produce any unusual results. At low heat fluxes ($Gr_m < 4.8 \times 10^5$, $Re < 320$) the effect of the grid spacer on the flow was to cause mixing in the region immediately downstream of the spacer. The streamlines (for laminar flow) would then redevelop at some distance downstream of the spacer. For greater heat fluxes, no laminar streamlines formed downstream of the spacer. The dye mixed thoroughly with the circulating fluid.

The average fluid friction results with and without grid spacers were practically the same (within experimental accuracy). These results were not surprising as the blockage ratio, ε, defined as

$$\varepsilon = \frac{A_{gs}}{A_{gs} + A_f} \quad (16)$$

where A_{gs} is the cross-sectional area of the spacers, was only $\varepsilon = 0.24$ so the additional flow resistance provided by the grid spacer was minimal.

The results obtained for the average heat transfer coefficients in the tests with grid spacers differed significantly from the results obtained in the tests without the grid spacers. At similar conditions (ie heating rates) the average heat transfer coefficients were increased by the grid spacers. Based on the empirical correlation given by Yao *et al*[17], the ratio of the local Nusselt number downstream of a grid spacer, Nu_{gs}, to the local Nusselt number which would exist if no grid spacer were present is

$$\frac{Nu_{gs}}{Nu} = 1.0 + 5.55\varepsilon^2 e^{-0.13(x/D_h)},$$

$$1 \times 10^4 < Re < 1.55 \times 10^5 \quad (17)$$

For the blockage ratio used in these experiments and for the spacing of the grid spacers, an increase of about 5% in the average Nusselt number for the grid spacer tests above the value obtained without the grid spacers is expected using Eq (17).

A plot of the heat transfer parameter $\overline{Nu}/Pr^{0.43}$ vs the Reynolds number for both counter-flow and parallel-flow arrangements has revealed a dependence of heat transfer coefficient on the flow regime[23]. At low Reynolds numbers ($Re < 100$), an increase of nearly 20% in the average Nusselt number is obtained due to the presence of the grid spacers. In the transition regime ($Re \cong 320$), an increase of only 10% is found[23]. That the heat transfer enhancement due to the grid spacers diminishes as the flow becomes mixed (irregular) is not surprising. This should be expected because the additional mixing resulting from the presence of the grid spacers would have a neglibie effect on the heat transfer as the fluid would already be well mixed.

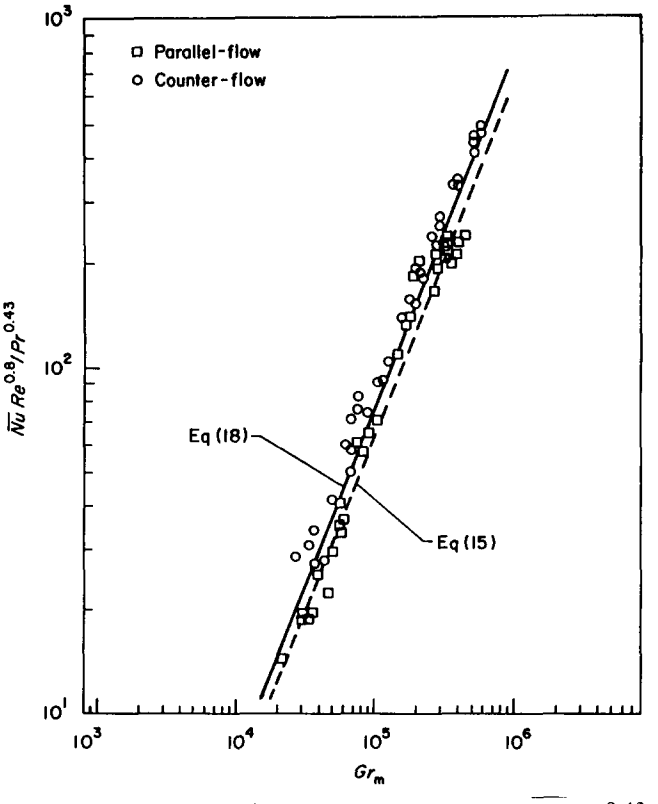

Fig 9 Comparison of heat transfer parameter $\overline{Nu}/Pr^{0.43}$ *for experiments without and with grid spacers on the tubes*

Plotting of the parameter $\overline{Nu}/Pr^{0.43}$ vs the modified Grashof number yielded a correlation similar to that shown in Fig 8, but there was somewhat more scatter of the experimental data than when plotting $\overline{Nu}/Pr^{0.43}$ vs Reynolds number[23]. Both the counter-flow and parallel-flow tests results were correlated by the empirical equation,

$$\overline{Nu} = 0.00055(Gr_m/Re)^{0.8} Gr_m^{0.2} Pr^{0.43} \quad (18)$$

The equation is of the same form as Eq (15) for the bundle without grid spacers, and differs only in the constant and the exponent of the modified Grashof number.

Conclusions

Based on the experimental results obtained, the following conclusions can be made.

1) The heating conditions investigated resulted in stable steady-state flows.
2) The natural circulation flow longitudinal to the test tube bundle was observed to be laminar when $Gr_m < 4.8 \times 10^5$ or when $Re < 340$. Above these values, radial mixing of the circulating fluid was observed. No recirculation of the flow at any of the thermal conditions studied was observed.

3) The frictional resistance was determined to be solely a function of the Reynolds number and was found to be predicted accurately by forced flow relations.
4) Heat transfer in the tube bundle was in a mixed-convection regime.
5) Empirical correlations for the average Nusselt number were developed. A more general correlation for relating $\overline{Nu}$ to Gr_m/Re is suggested.
6) The grid spacers used in this study ($\varepsilon = 0.24$) had no discernible effect on the fluid friction factors. However, they were found to enhance the average heat transfer coefficients over those which would be present without grid spacers, especially in the laminar flow regime.

Acknowledgements

The work described in the paper was supported, in part, by Argonne National Laboratory under Contract No 31-109-38-6959 and US Nuclear Regulatory Commission Grant No NRC-G-04-006.

References

1. **McKee H. R.** Thermosyphon reboilers: a review. *Ind. Eng. Chem., 1970*, **62**, *76–82*
2. **Japikes D.** Advances in thermosyphon technology. *In Advances in Heat Transfer, Academic Press, New York, 1973, Vol 9, 1–111*
3. **Norton B. and Probert S. D.** Natural-circulation solar-energy stimulated systems for heating water. *Applied Energy, 1982*, **11**, *167–196*
4. **Zvirin Y.** A review of natural circulation loops in pressurized water reactors and other systems. *Nuclear Engng. and Design, 1981*, **67**, *203–225*
5. **Mertal A. and Greif R.** A review of natural circulation loops. *Advanced Study Institute Proceedings on Natural Convection: Fundamentals and Applications, July 1984, Izmir, Turkey*
6. **Zvirin Y. and Rabinoviz Y.** *Modeling of Natural Circulation Phenomena in Nuclear Reactor Cooling Loops. Electric Power Research Institute Report NP-2951, 1983*
7. **Gruszczynski M. J. and Viskanta R.** *Heat Transfer to Water From a Vertical Tube Bundle Under Natural Circulation Conditions. Argonne National Laboratory, Report No ANL-83-7, 1983*
8. **Zvirin Y., Heuck P. R. III, Sullivan C. W. and Duffey R. B.** Experimental and analytical investigation of a natural circulation system with parallel loops. *J. Heat Transfer, 1981*, **103**, *645–652*
9. **Damerell P. S. and Schoenhals R. J.** Flow in a toroidal thermosyphon with angular displacement of heated and cooled sections. *J. Heat Transfer, 1976*, **101**, *672–676*
10. **Sparrow E. M. and Loeffler A. L.** Longitudinal laminar flow between cylinders arranged in regular arrays. *AIChE Journal, 1959*, **5**, *325–330*
11. **Schmid J.** Longitudinal laminar flow in an array of circular cylinders. *Int. J. Heat and Mass Transfer, 1966*, **9**, *925–937*
12. **Mohanty A. K. and Roy D. K.** Fluid flow through a circular tube containing rod cluster. *in Fluid Flow and Heat Transfer over Rod or Tube Bundles, ed S. Yao and P. Pfund, ASME, New York, 1971, 121–128*
13. **Johannsen K.** Longitudinal flow over tube bundles. *in Low Reynolds Number Flow Heat Exchangers, ed S. Kakac et al, Hemisphere Publishing Corp., Washington, DC, 1983, 229–273*
14. **Johannsen K.** Heat exchangers having longitudinal flow over tubes or rods. *in Low Reynolds Number Flow Heat Exchangers, ed S. Kakac et al, Hemisphere Publishing Corp., Washington, DC, 1983, 275–297*
15. **Marek J. and Rehme K.** Heat transfer in smooth and roughened rod bundles near spacer grids. *in Fluid Flow and Heat Transfer over Rod or Tube Bundles, ed S. Yao and P. Pfund, ASME, New York, 1979, 163–170*
16. **Bragina O. N., Lel'chuck V. L., Sorokin A. G. and Shuyskaya K. F.** Experimental study of enhancement of heat transfer from a tube bundle in turbulent axial flow. *Heat Transfer – Soviet Research, 1981*, **13** (*4*), *14–18*
17. **Yao S. C., Hochreiter L. E. and Leech W. J.** Heat transfer augmentation in rod bundles near grid spacers. *J. Heat Transfer, 1982*, **104**, *76–81*
18. **Grober H., Erk S. and Grigull H.** *Fundamentals of Heat Transfer. McGraw Hill Book Co. Inc., New York, 1961*
19. **Kreith F.** *Principles of Heat Transfer. Intext Press, Inc., New York, 1973*
20. **Metalis B. and Eckert E. R. G.** Forced, mixed and free convection regimes. *J. Heat Transfer, 1964*, **86**, *295–296*
21. **Welander P.** On the oscillatory instability of a differentially heated fluid loop. *J. Fluid Mech., 1967*, **29**, *17–30*
22. **Gabitto J. P. and Boehm U.** Experimental study of free convective mass transfer in porous media. *Int. J. Heat Mass Transfer, 1981*, **24**, *1675–1679*
23. **Hallinan, K. P.** *Heat Transfer from a Vertical Tube Bundle in a Natural Circulation Loop. MSME Thesis, Purdue University, W. Lafayette, Indiana, USA, 1983*